Design, synthesis and in vitro evaluation of β-glucuronidase-sensitive prodrug of 5-aminolevulinic acid for photodiagnosis of breast cancer cells

Herceg, Viktorija; Adriouach, Souad; Janikowska, Karolina; Allémann, Eric; Lange, Norbert; Babic, Andréj

How to cite

HERCEG, Viktorija et al. Design, synthesis and in vitro evaluation of β-glucuronidase-sensitive prodrug of 5-aminolevulinic acid for photodiagnosis of breast cancer cells. In: Bioorganic Chemistry, 2018, vol. 78, p. 372–380. doi: 10.1016/j.bioorg.2018.03.020

This publication URL: https://archive-ouverte.unige.ch/unige:104599
Publication DOI: 10.1016/j.bioorg.2018.03.020

Design, synthesis and *in vitro* evaluation of β-glucuronidase-sensitive prodrug of 5-aminolevulinic acid for photodiagnosis of breast cancer cells

Herceg V.[1], Adriouach S.[1], Janikowska K., Allémann E., Lange N., Babič A.*

School of Pharmaceutical Sciences

University of Geneva, University of Lausanne

Rue Michel Servet 1, CH-1211 Geneva 4, Switzerland

Abstract

Treatment of cancer cells by clinically approved hexyl ester of 5-aminolevulinic acid (ALA-Hex) induces accumulation of fluorescent porphyrins in tumors. This allows fluorescence photodiagnosis (PD) of bladder cancer by blue light illumination. However, PD of other cancers is hampered by acute toxicity of the compound limiting its use to local applications. We have designed and synthesized a new prodrug of ALA-Hex that tackles the stability-activity paradox of amino-modified 5-ALA prodrugs. The glucuronide prodrug Glu-ALA-Hex demonstrates excellent stability under physiological conditions and activation in the presence of the target enzyme. β-glucuronidase-triggered release of 5-ALA is programmed to yield fluorescence in tumor environment with elevated β-glucuronidase activity, a characteristic of many solid tumors. Glu-ALA-Hex produces similar levels of fluorescence as ALA-Hex in breast cancer MCF7 cells *in vitro* but with much lower non-specific cell toxicity.

Keywords 5-aminolevulinic acid, prodrugs, beta-glucuronidase, fluorescence, photodiagnosis, breast cancer

1. Introduction

5-aminolevulinic acid (5-ALA) is a precursor of heme present in the majority of human cells. However, when applied to tumors, a photosensitizer protoporphyrin IX (PpIX) is overproduced and accumulated within cancer cells. This is thought to be due to aberrant negative-feedback mechanisms caused by the dysregulation of enzymes involved in the heme biosynthesis, although the underlying mechanisms are not completely understood [1]. PpIX induced by the treatment with 5-ALA therefore allows photodiagnosis (PD), an emerging modality for cancer detection prior to resection [2]. This fluorophore emits red light fluorescence under visible blue light irradiation, enabling identification of tumor tissue with millimeter accuracy otherwise visually undistinguishable from normal tissue.

* corresponding author: Tel. +41 22 379 36 78, Fax. +41 22 37 965 67.
Email: andrej.babic@unige.ch
Address: School of Pharmaceutical Sciences, Rue Michel Servet 1, 1211 Geneva, Switzerland
[1] Both authors contributed equally to this work.

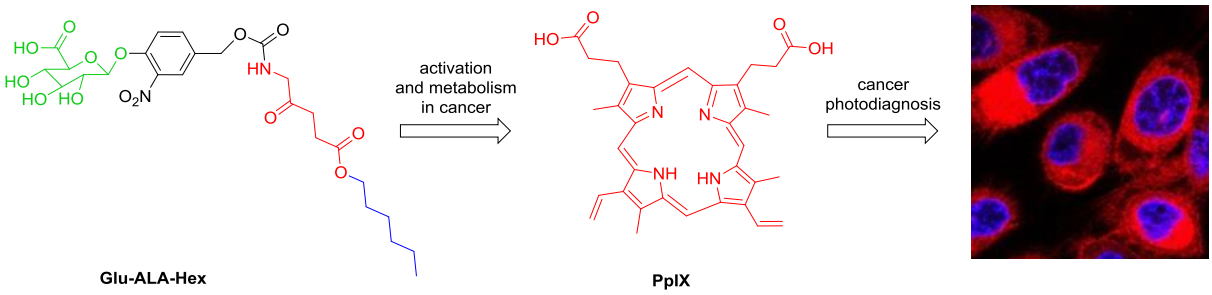

Figure 1. Structural elements incorporated into β-glucuronidase-sensitive 5-ALA double prodrug Glu-ALA-Hex (left). Glucuronic acid (green) was attached through a self-immolative linker (black) to 5-aminolevulinic acid (red) hexyl ester (blue). Cancer cells metabolize the prodrug to PpIX (center) which allow PD of cancer cells (right).

Conventional photosensitizers (PS) also allow tumor PD, however, 5-aminolevulinc acid (5-ALA)-based interventions offer excellent tumor specificity with reduced photosensitivity reactions caused by PS accumulation in non-targeted tissues. In 5-ALA-based therapies this side-effect is much less pronounced as a consequence of PpIX metabolism into endogenous non-fluorescent heme. This has led to the clinical use of 5-ALA, utilized as a PD surgical aid in high-grade gliomas resections [3]. The more lipophilic hexyl ester of 5-ALA has also been approved for local application to detect early human bladder cancer [4, 5]. The continuing development of 5-ALA in oncology has led to trials in PD of gastric cancer [6], gastric cancer lymph nodes metastases [7], cervical intraepithelial neoplasia [8], ovarian cancer metastases [9] and also cancer stem cells [10]. Except for the use in PD of gliomas, 5-ALA has to be applied topically due to the unfavorable pharmacokinetics of the molecule [11].

Attempts to improve the drug-like properties of the molecule have mostly focused on prodrug approaches. Most of the research has been focused on the modification of carboxylic group yielding a wide variety of esters of 5-ALA [12]. Eggleston and colleagues were the first to design double prodrugs of 5-ALA, where the amino group was derivatized with various N-acetyl amino acids. However, the 5-ALA peptide derivatives only show significant PpIX production in cell lines that express acyl peptide hydrolase [13]. We have recently reported two new phosphatase-sensitive double prodrug classes of 5-ALA with tunable release kinetics and robust fluorescence profiles in U87MG glioblastoma cancer cells [14]. This work has paved the way towards less toxic 5-ALA prodrugs. It demonstrates the feasibility of 5-ALA amino group chemical modification whilst retaining the pharmacological activity in cancer cells which is lacking in most other 5-amino modified derivatives of 5-ALA [15]. The discovery of novel 5-ALA double prodrugs is a way to progress 5-ALA-based PD as means of precise tumor detection.

To this end, β-glucuronidase-sensitive prodrugs of 5-ALA could yield a new cancer detection strategy. β-glucuronidase is a tetrameric enzyme from glycosidase family localized in cell lysosomes [16]. Its physiological role is the hydrolysis of glucuronic acid-containing complex carbohydrates, such as glycosaminoglycans like chondroitin sulfate, heparan sulfate and dermatan sulphate [17]. Fishman and Anylan were the first to report the elevated activity of β-glucuronidase in tumor cells [18]. Their observations were further confirmed by others who found the elevated β-glucuronidase expression in microenvironment of lung, breast, ovarian, gastrointestinal cancer and melanomas [19-22]. The concept of β-glucuronidase-sensitive prodrugs was first suggested by Tietze [23]. Since then, various cytotoxic agents including anthracyclines [21, 24-27], taxanes [28, 29], 5-fluorouracil [30], campothecin [31-34] have been converted into β-glucuronidase-sensitive prodrugs liberated in solid tumors. The main aim of these modifications is reducing toxicity and targeted release of active principle.

Herein, we report the design, synthesis and *in vitro* evaluation of β-glucuronidase-sensitive prodrug of 5-ALA (Glu-ALA-Hex) for PD of cancers. The PD potential of the novel double prodrug was assessed by fluorescence-induction and confocal fluorescence microscopy after incubation with Glu-ALA-Hex in MCF7 breast adenocarcinoma cells.

2. Results and Discussion

2.1. Design

Prodrugs of 5-ALA have to successfully overcome the so-called stability-activity paradox of 5-ALA.[14] It stems from the fact that the prodrugs of 5-ALA with free amino group are unstable under physiological conditions [35]. Conversely, when the prodrug moiety is introduced to the same amino group, the prodrugs must be cleaved before entering the haem biosynthetic pathway to yield tetrapyrrolic porphyrins such as PpIX. This hypothesis is supported by experiments where 5-ALA amides generally fail to induce clinically relevant fluorescence of PpIX *in vitro* and *in vivo* in the absence of specific peptidases [36, 37]. Moreover, Berg and colleagues have shown that even a N-formyl ALA derivative failed to induce porphyrin synthesis [38].

Glu-ALA-Hex construct (Figure 1) combines β-glucuronic acid trigger and 5-ALA in the form of hexyl ester (ALA-Hex). Both moieties are connected by a self-immolative 4-hydroxy-3-nitrobenzyl spacer attached to 5-ALA by carbamate group [39]. The whole construct needs to be stable under physiological conditions yet enzyme-sensitive. Rapid conversion by tumor β-glucuronidase yields sufficient amounts of 5-ALA for fluorescence PD. β-glucuronidase-sensitive prodrugs employing spacer groups between the active and the prodrug moieties have shown improved activation, drug-release and overall performance [40-43]. The combined enzymatic-chemical mechanism of Glu-ALA-Hex activation is

presented in Figure 2. Tumor-specific cleavage by β-glucuronidase present in several cancers should further raise the level of tumor specificity of PD.

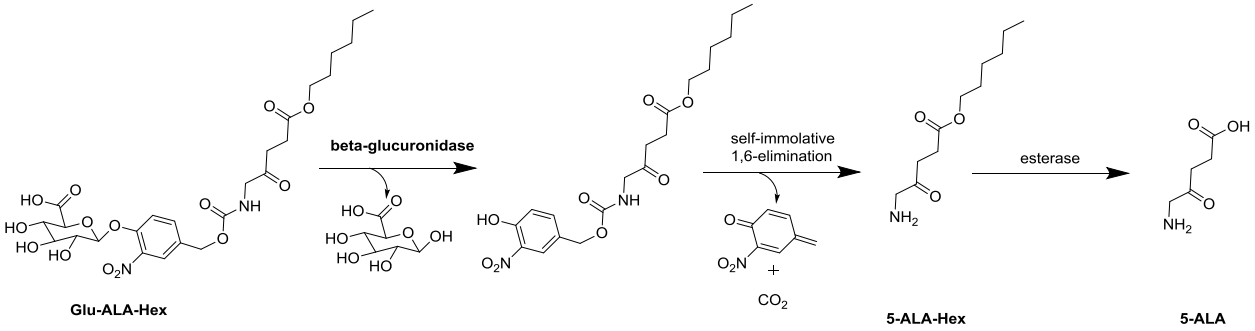

Figure 2. The mechanism of Glu-ALA-Hex activation. β-glucuronidase triggers spontaneous cleavage of self-immolative linker by 1,6-elimination. Once released, ALA-Hex efficiently enters the cells and is cleaved by esterases to yield 5-ALA.

2.2. Chemistry

The target molecule was synthesized in 7-steps (Scheme 1). The starting D-glucuronolactone was reacted with sodium metoxide in dry methanol followed by acetylation by acetic anhydride according to the procedure by Chern and colleagues to afford protected carbohydrate **1** [31]. Methyl 1,2,3,4-tetra-acetyl-D-glucopyranuronate **1** was brominated with $TiBr_4$ and reacted without purification with 4-hydroxy-3-nitro-benzaldehyde in the presence of Ag_2O to yield D-glucuronyl derivative **2** in modest 44% yield. As reported the reaction afforded the *β*-anomer selectively [44]. The aldehyde **2** was reduced by $NaBH_4$ to benzyl alcohol derivative **3** in 72% yield. Under these reduction conditions the aromatic nitro group of the linker system was stable. Next, the ALA-Hex was introduced into the construct by 2-step one-pot procedure. First, **3** was activated with *N,N′*-disuccinimidyl carbonate which afforded N-succimidyl carbonate which was reacted in the second step with 2 eq. of ALA-Hex **4** to afford the fully protected compound **5** in very good yield (83 %). The final deprotection of **5** proved demanding since the molecule contains carbamate, glycoside and several ester bonds. The construct needs to contain these relatively liable bonds to ensure robust conversion into 5-ALA followed by the mitochondrial biosynthesis into fluorescent PpIX. Some of the tested conditions that failed to deprotect **5** included NaOMe/MeOH, aqueous LiOH, NaOH, Na_2CO_3 in MeOH and aqueous K_2CO_3. The total deprotection caused transesterification or degradation of the whole construct as detected by LC-MS. Finally, the successful deprotection was achieved using aqueous solution of MeOH and TEA at 70 °C for 2h. The Glu-ALA-Hex **6** was obtained after semi-preparative HPLC purification in good yield.

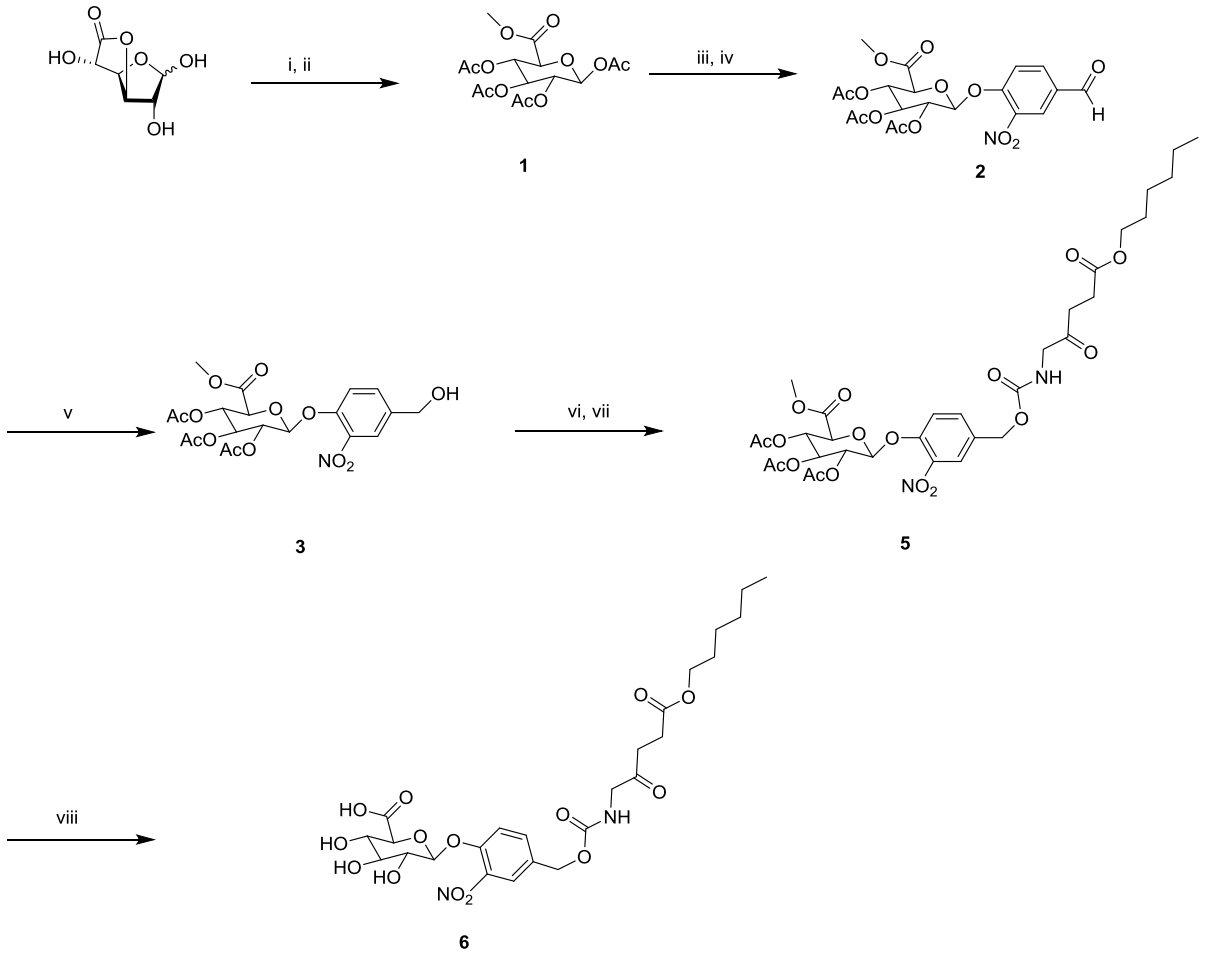

Scheme 1. Chemical synthesis of β-glucuronidase-sensitive double prodrug Glu-ALA-Hex. Reagents and conditions: (i) NaOMe, MeOH, r.t., 1 h; (ii) Ac_2O, $HClO_4$, r.t., 4 h; (iii) $TiBr_4$, DCM, r.t., 24 h; (iv) Ag_2O, 4-hydroxy-3-nitro-benzaldehyde, CH_3CN, r.t., 4 h; (v) $NaBH_4$, DCM, MeOH, 0 °C, 30 min; (vi) *N,N′*-disuccinimidyl carbonate, TEA, CH_3CN, DMF, r.t., 1 h; (vii) hexyl 5-amino-4-oxopentanoate hydrochloride (**4**), TEA, 0 °C to r.t., 3 h; (viii) TEA, MeOH, H_2O, 70 °C, 2 h.

2.3. Enzymatic activation

Glu-ALA-Hex is designed to release 5-ALA specifically in the presence of β-glucuronidase in the tumor tissues. Following the rate-limiting enzymatic removal of glucuronic acid, the self-immolative linker cleaves spontaneously to give the ALA-Hex (Figure 2). The latter reaction is a 1,6-benzyl elimination reaction which proceeds rapidly [45].

The sensitivity of the novel ALA prodrug **6** to β-glucuronidase cleavage was assessed *in vitro*. The enzyme-triggered release of ALA-Hex was efficient with a half-life around 10 min at the enzyme concentration of 1 U/mL (Figure 3a). In terms of stability, the double prodrug construct proved very stable at physiological conditions showing no degradation in 12 h at 37 °C. Conversely, ALA-Hex shows

propensity to irreversible dimerization with limited stability under physiological conditions (Figure 3b) [14]. These results confirmed the validity of the design, namely the use of an appropriate short self-immolative linker between the 5-ALA and glucuronic acid. Keeping in mind that relatively high doses of 5-ALA are needed to produce tumor fluorescence *in vivo*, the release profile was in line with desired release characteristics.

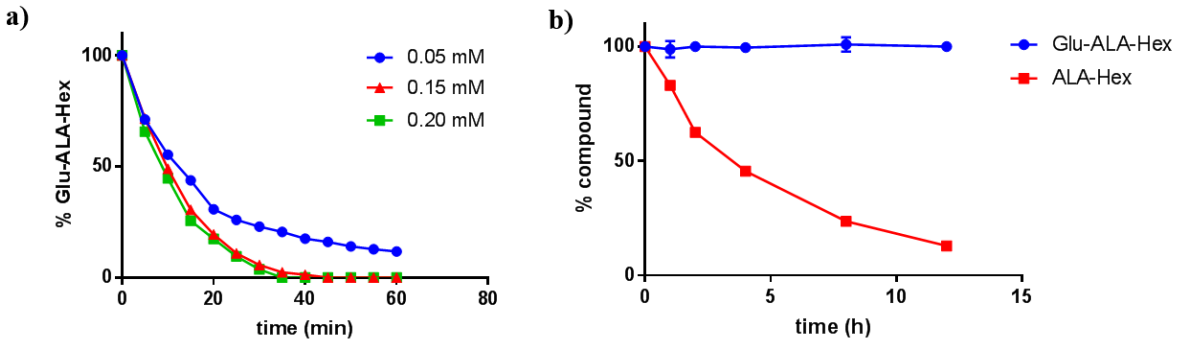

Figure 3. Glu-ALA-Hex activation assay and stability. a) Kinetics of prodrug activation in the presence of 1 U/mL of β-glucuronidase at pH=6.8 at different substrate concentrations; b) The stability profile of Glu-ALA-Hex compared to ALA-Hex at physiological pH.

2.4. Dark toxicity

5-ALA derivatives produce PpIX photosensitizer, capable of producing singlet oxygen upon light-irradiation in cancer cells. Hence non-specific toxicity was assessed in the absence of light to avoid light-induced photodynamic effects. Glu-ALA-Hex did not affect the viability of MCF7 breast cancer cells at any tested concentration (Figure 4, blue columns). In contrast, ALA-Hex which forms a part of Glu-ALA-Hex construct caused complete cell death at 2.0 mM and above. This was in agreement with published data on the cell toxicity of ALA-Hex [14, 15] and is the reason why ALA-Hex is not approved for systemic use. Very promisingly, Glu-ALA-Hex displayed limited cytotoxicity in the dark, even in the presence of β-glucuronidase, where ALA-Hex was produced *in situ*.

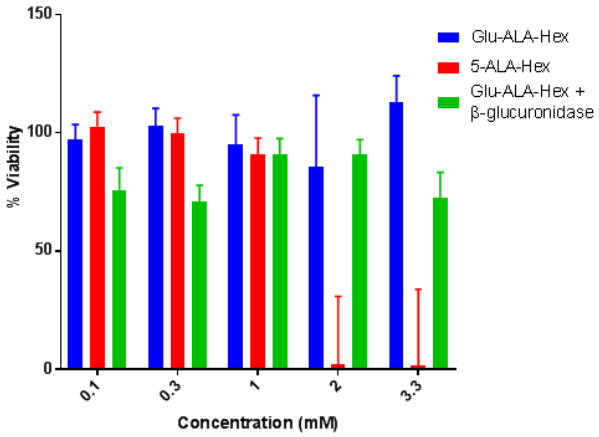

Figure 4. Dark toxicity in MCF7 cells incubated with increasing concentrations of Glu-ALA-Hex (green), ALA-Hex (red) and Glu-ALA-Hex in the presence of β-glucuronidase (blue). N=3 ± s.d.

2.5. PpIX fluorescence induction *in vitro*

Glu-ALA-Hex induced very low PpIX fluorescence in MCF7 cells in the absence of β-glucuronidase (Figure S1). This was hardly surprising since Glu-ALA-Hex is a synthetic conjugate of ALA-Hex and glucuronic acid and glucuronation generally speaking decreases biological activity of drugs, making them less toxic than their parent drugs. This is demonstrated by several β-glucuronidase-sensitive prodrugs [24-26, 31-33, 46-48]. However, low induction of PpIX synthesis by Glu-ALA-Hex in monolayer cells *in vitro* is not representative of tumor microenvironment *in vivo*.

It is well established that solid tumors, including breast, lung and gastrointestinal tract carcinomas, as well as melanomas have increased expression of β-glucuronidase as compared to normal tissues [22]. β-glucuronidase is present mainly in necrotic areas of the tumors. After cell necrosis, the liberation of lysosomal β-glucuronidase and the infiltration with activated neutrophils leads to increased levels of the enzyme in the extracellular matrix of the malignant tissues [49, 50]. As it was reported previously, *in vitro* incubation of β-glucuronidase-sensitive prodrugs of epirubicin, daunorubicin and doxorubicin with cancer cells did not lead to the complete release of the active compound [26, 51]. However, increased activity was observed when β-glucuronidase-sensitive prodrugs of daunorubicin or doxorubicin were incubated with cells in presence of an excess of active enzyme indicating complete liberation of the cytotoxic drugs [24, 51].

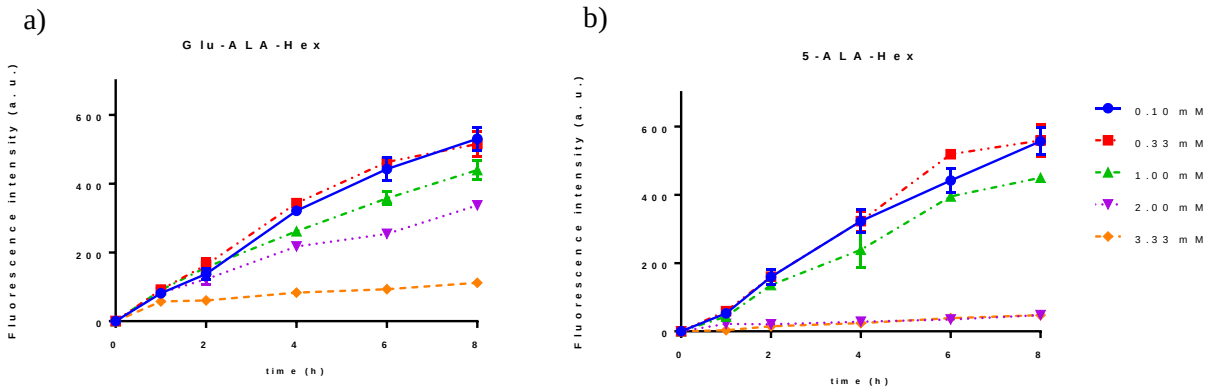

Figure 5. β-glucuronidase-triggered fluorescence production in MCF 7 breast cancer cells. PpIX fluorescence was measured at different time points over 24 h by incubation with different concentrations of Glu-ALA-Hex (a), and ALA-Hex reference (b) in the presence of β-glucuronidase. N=3 ± s.d.

We simulated the necrotic tumor microenvironment *in vitro* by the presence of β-glucuronidase with the MCF7 cells. In this case, fluorescence was observed at all tested concentrations of Glu-ALA-Hex (0.1 – 3.3 mM) with a predictable decrease in fluorescence at the highest 3.3 mM concentration (Figure 5). Furthermore, no lag in fluorescence kinetics with nearly identical fluorescence levels to ALA-Hex were observed. However, ALA-Hex displayed concentration dependant on-off characteristics with a distinct drop off of fluorescence above 1.0 mM, a consequence of pronounced non-specific cell toxicity.

Live cell imaging provided direct evidence of PpIX induction in MCF7 cells (Figure 6). However, PpIX is a photosensitizer that photobleaches very rapidly making its detection by conventional confocal microscopy difficult compared to two-photon excitation fluorescence microscopy [52, 53]. Minimum laser power and very fast image acquisitions had to be employed for PpIX fluorescence images. Nevertheless, diffuse red PpIX fluorescence could be detected within the cells when Glu-ALA-Hex was incubated with MCF7 cells in the presence of β-glucuronidase (Figure 6b). Similar diffuse localization pattern of PpIX was detected for ALA-Hex. Partial co-localization with Mitotracker green indicated mitochondrial localization of PpIX which is in accordance with published data indicating mitochondria and endoplasmatic reticulum as main PpIX cellular distribution organelles [15, 52]. Our experiments also confirmed that PPIX does not co-localize with lysosomes (Figure S2). It is noteworthy that some cells displayed apparent nuclear localization of PPIX (Figure 6b and 6c). This is likely an experimental artefact as a consequence of the very weak fluorescence signal of PPIX. Therefore slight crosstalk between Hoechst 33342 and PPIX channels could not be avoided under the experimental conditions used.

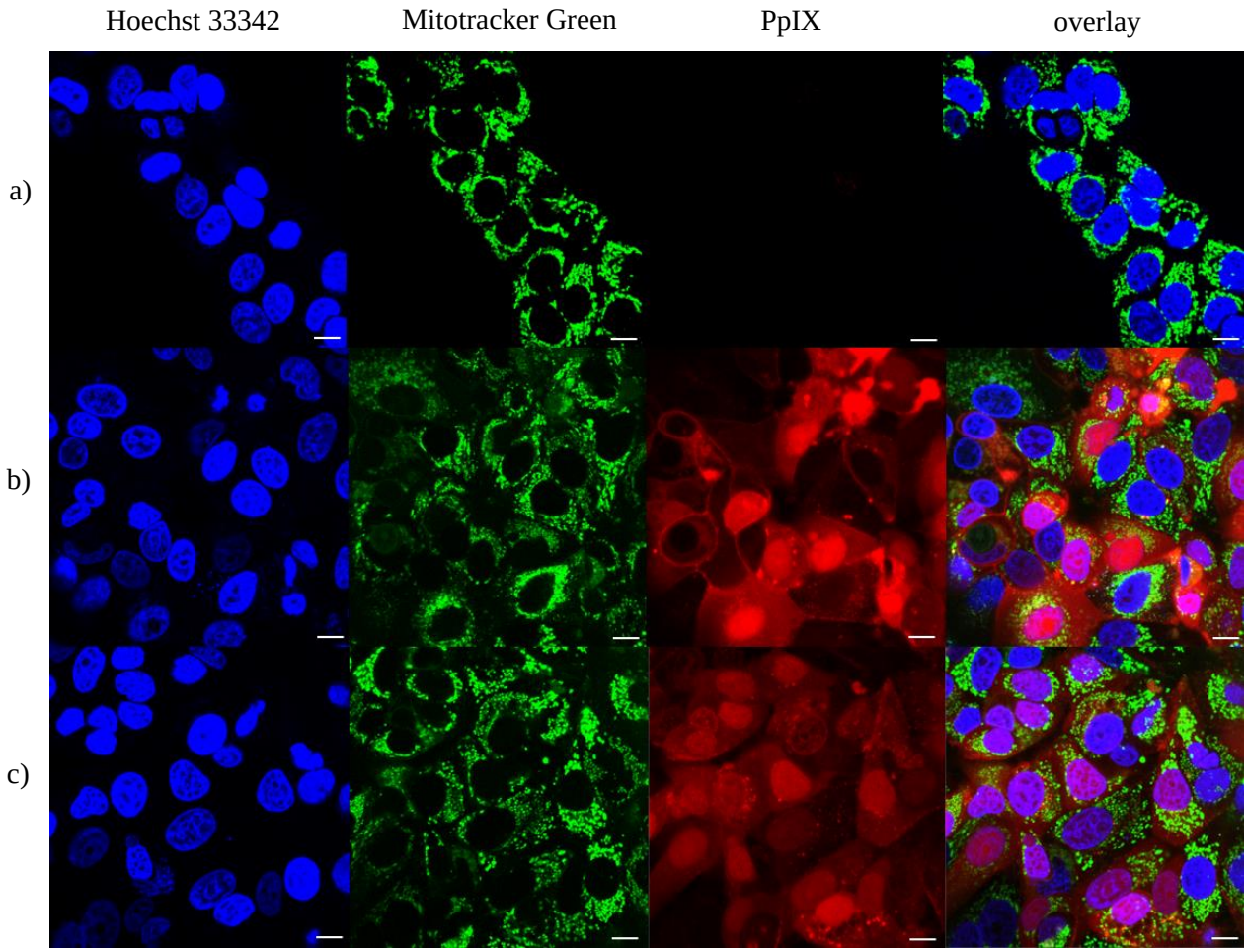

Figure 6. Confocal scanning micrographs of live MCF7 cells incubated with 0.33 mM Glu-ALA-Hex (a), Glu-ALA-Hex in the presence of β-glucuronidase (b), ALA-Hex (c). The cells were co-stained with Hoechst 33342 for nuclei (blue) and Mitotracker green for mitochondria (green). PpIX fluorescence (red). Scale bar 10 µm.

3. Conclusion

Glu-ALA-Hex was designed as β-glucuronidase-sensitive 5-ALA double prodrug. It was successfully synthesized and characterized. It demonstrated excellent stability under physiological pH and good sensitivity as β-glucuronidase substrate. Compared to the acutely toxic ALA-Hex, it had low dark toxicity for MCF7 cells. Glu-ALA-Hex demonstrated the capability of fluorescence switch by incorporating tumor specific β-glucuronidase drug release trigger. Glu-ALA-Hex induced the fluorescence in MCF7 breast cancer cells only in the presence of β-glucuronidase. Further development of the new 5-ALA prodrug could lead to highly specific PD of tumors with unprecedented levels of tumor specificity as invaluable aid in surgical resections of cancer.

4. Experimental

4.1. General

All chemicals were obtained from Acros Organics (Basel, Switzerland) and Sigma-Aldrich (Buchs, Switzerland) and used without further purification. β-Glucuronidase (EC 3.2.1.31) was purchased from Sigma-Aldrich. Phosphate Buffer Saline (PBS) pH 7.4 was purchased from Invitrogen (Zug, Switzerland). Deuterated NMR solvents were obtained from Cambridge Isotope Laboratories (Tewksbury, USA). Tetrahydrofuran (THF), *N*,*N*,-dimethylformamide (DMF) and dichloromethane (DCM) were obtained by Inert PureSolv Micro (Amesbury, USA) alumina column based solvent drying system. All other solvents used were HPLC grade. N,N-dimethylformamide (DMF), methanol (CH_3OH), diethyl ether (Et_2O) and acetone were purchased from Sigma-Aldrich (Buchs, Switzerland). Ethyl acetate (AcOEt) was purchased from Biosolve (Dieuze, France), and acetonitrile (CH_3CN) was supplied by Carlo Erba Reagents (Balerna, Switzerland). The water used was deionized by a Milli-Q lab water system (Millipore, Molsheim, France).

Reactions were performed under anhydrous conditions using standard syringe-septa techniques under a positive pressure of nitrogen. Thin layer chromatography (TLC) was performed with aluminium backed silica plates (Merck-Keiselgel 60 F254) with a suitable mobile phase and visualized using a UV fluorescence lamp (254 and 366 nm) and/or developed with nihydrin, sulfuric acid (20%), 2,4-dinitrophenylhydrazine or phosphomolybdic acid (PMA). Flash chromatography was performed on an automated PuriFlash® 4100 machine from Interchim (Montlucon, France) using Interchim silica columns puriFlash® HP 30 µm equipped with a PDA detector (200 – 800 nm) and automated fraction collector. The elution profile was monitored using Flash Interchim software version 5.0x. Semi-preparative HPLC column was performed on a Shimadzu binary high-pressure gradient LC system equipped with a DAD detector and automated fraction collector using Nucleodur C18-Htec 5 µm (250×21 mm) semi-preparative column from Macherey-Nagel (Duren, Germany). Full gradient of 1-100% AcN/H2O + 0.01% TFA was used unless otherwise noted. Analytical UPLC was conducted using Thermo Fischer UPLC system equipped with a PDA detector (200 – 800 nm) and temperature-controlled auto-sampler and fitted with Macherey-Nagel EC50/2 Nucleodur Gravity 1.8 µm column (50 x 2.1 mm). ^{1}H and ^{13}C NMR spectra were recorded on Varian Gemini 300 MHz, Varian Innova 500 MHz or Bruker Avance III Cryo 600 MHz spectrometers at 298 K. Chemical shifts (δ) are quoted in parts per million (ppm) and coupling constants (J) are in hertz (Hz). s stands for singlet, d for doublet, dd for doublet of doublets, t for triplet, q for quartet, m for multiplet. Residual solvent peaks were used as the internal reference for the proton and carbon chemical shifts. NMR spectra were processed with Mnova version 10.0.2 software package. Low resolution mass spectrometry (LRMS) was carried out on a HTS PAL-LC10A – API 150Ex and Advion Expression CMS-L instruments using electrospray ionization (ESI) in

positive and negative modes. High resolution mass spectrometry (HRMS) was carried out on a QSTAR Pulsar (AB/MDS Sciex) instrument in ESI (positive mode). LRMS spectra were analyzed by Advion Data Express software v. 3.1.21.1. Matrix-assisted laser desorption/ionisation-Time of flight (MALDI-TOF) mass spectra were obtained using an Axima CFR+ (Shimadzu) with a cyano-4-hydroxycinnamic acid (CHCA) matrix in linear or reflectron mode. MALDI spectra were processed using Shimatzu Biotech LaunchPad version 2.8 software. Chemical structures were drawn and named according IUPAC nomenclature using ChemBioDraw Ultra version 14.0.0.117 software package. The pH was measured on a Metrohm 691 pH meter using a spearhead electrode (Zofingen, Switzerland), calibrated with Metrohm buffers.

Figures and statistical analysis were done using GraphPad Prism 7.02, 2017, (GraphPad Software Inc.) software. P-values < 0.05 were considered as statistically significant.

4.2. Synthesis

Methyl 1,2,3,4-tetra-acetyl-D-glucopyranuronate (1). Compound **1** was synthesized according to published procedure [31]. Briefly, D-(+)-glucuronic acid γ-lactone (17.6 g, 0.100 mol) was suspended in dry methanol (100 mL). After addition of sodium methylate (0.15 g, 30 wt. %) the reaction mixture was stirred at ambient temperature. After 60 min methanol was removed under reduced pressure yielding a brownish syrup. Acetic acid anhydride (80 mL, 0.66 mol) and $HClO_4$ (0.3 mL) were added to the syrup and stirred for 4h. The reaction mixture was stored at 4° overnight and then suction filtered. The filtrate was poured onto ice and neutralized with $NaHCO_3$. After suction filtering the filtrate was extracted with DCM. The organic phase was washed with brine, dried over Na_2SO_4 and concentrated under reduced pressure. The obtained syrup slowly crystalized at 4 °C yielding a total of 22.9 g (60.9 mmol, 60.9 %). ^{1}H NMR (300 MHz, DMSO-*d*$_6$) δ 5.99 (d, *J* = 8.1 Hz, 1H), 5.55 – 5.41 (m, 2H), 5.17-5.10 (m, 2H), 5.04 – 4.90 (m, 2H), 4.65 (d, *J* = 9.8 Hz, 1H), 3.61 (s, 3H), 2.07-2.04 (m, 6H), 2.01 (s, 3H), 1.98-1.97 (s, 3H). ^{13}C NMR (75 MHz, DMSO-*d6*) δ ^{13}C NMR (75 MHz, cdcl$_3$) δ 170.28, 170.10, 169.62, 169.38, 98.80, 91.53, 81.84, 78.28, 76.39, 73.16, 71.99, 70.31, 69.10, 68.29, 53.24, 20.99, 20.76, 20.68, 20.12. LRMS (ESI): m/z calculated for $[M+NH_4]^+$ 394.1, found 394.0.

Methyl 1-(4-formyl-2-nitrophenyl)-2,3,4-triacetyl-*β*-D-glucopyranuronate (2). A solution of **1** (1.00 g, 2.66 mmol) and $TiBr_4$ (1.17 g, 3.19 mmol) in DCM (30 mL) was stirred at ambient temperature. After 24 h the organic phase was washed with cold solution of $NaHCO_3$ and dried over Na_2SO_4. Yellow oil was obtained after evaporation to dryness. The oil was dissolved in AcN (100 mL) before the addition of Ag_2O (712 mg, 3.07 mmol) and 4-hydroxy-3-nitro-benzaldehyde (400 mg, 2.40 mmol). After 4 h the black reaction mixture was filtered, evaporated to dryness. The crude product was purified by Flash chromatography using hexane/ethyl acetate 1/1 as mobile phase yielding colorless solid (565 mg, 44.0

%). 1H NMR (300 MHz, $CDCl_3$) δ 9.92 (s, 1H), 8.27 (d, J = 2.0 Hz, 1H), 8.06 (dd, J = 8.7, 2.1 Hz, 1H), 7.48 (d, J = 8.6 Hz, 1H), 5.45 – 5.25 (m, 5H), 4.33 (d, J = 8.2 Hz, 1H), 3.67 (s, 3H), 2.08 (s, 3H), 2.03 (m, 6H). 13C NMR (75 MHz, CDCl3) δ 189.07, 170.18, 169.57, 169.38, 166.92, 153.47, 141.16, 134.65, 131.55, 126.85, 118.78, 101.45, 98.64, 82.19, 78.88, 76.06, 72.71, 70.42, 69.89, 69.13, 68.36, 53.32, 20.76, 20.71. LRMS (ESI): m/z calculated for $[M+NH_4]^+$ 501.1, found 500.8.

Methyl 1-(4-hydroxymethyl-2-nitrophenyl)-2,3,4-triacetyl-*β*-D-glucopyranuronate (3). Compound **2** (232 mg, 0.48 mmol) was dissolved in DCM (10 mL) and MeOH (10 mL) and cooled to 0 °C. $NaBH_4$ (30 mg, 0.72 mmol) was added slowly to the reaction mixture. After 30 min NH_4Cl (20 mL) was added and extracted with DCM (3x15 mL). The organic phase was dried with Na_2SO_4 and evaporated to dryness. The crude product was purified by Flash chromatography using DCM/MeOH gradient yielding colorless solid (168 mg, 0.35 mmol, 72.0 %). ^{1}H NMR (500 MHz, CD_3CN) δ 7.76 (d, *J* = 2.1 Hz, 1H), 7.54 (dt, *J* = 8.7, 2.1, 1.9 Hz, 1H), 7.38 (d, *J* = 8.6 Hz, 1H), 5.49 – 5.33 (m, 2H), 5.31 – 5.14 (m, 2H), 4.58 (s, 2H), 4.41 (d, *J* = 9.8 Hz, 2H), 3.67 (s, 3H), 2.02 (s, 3H), 2.01 (s, 3H), 1.99 (s, 3H). ^{13}C NMR (126 MHz, Acetonitrile-d_3) δ 170.03, 169.89, 169.44, 167.30, 147.88, 138.52, 132.19, 122.90, 118.49, 117.61, 99.32, 72.13, 71.18, 70.36, 69.06, 62.31, 52.75, 20.11, 20.07, 20.03.

Hexyl 5-amino-4-oxopentanoate hydrochloride (4). Compound **4** was synthesized using modified published procedures [14, 54]. Briefly, thionyl chloride (8.20 g, 68.9 mmol) was added dropwise to 1-hexanol (60.0 mL, 48.8 g, 475 mmol) at 0 °C. After stirring for 10 min the ice-bath was removed, and 5-aminolevulinic acid hydrochloride (8.20 g, 49.0 mmol) was added. The reaction mixture was stirred at ambient temperature for 1 h, followed by reflux at 80 °C. After 2 h the reaction mixture was cooled down and ether (150 mL) was added. The precipitate was filtered off and washed with ether (2 × 50 mL). Extensive drying in vacuo gave colorless solid (10.6 g, 42.1 mmol, 86%). 1H NMR (300MHz, DMSO-d_6) δ 8.35 (s, 3H), 3.97 (t, J=6.7 Hz, 2H), 3.92 (s, 2H), 2.78 (t, J = 6.5 Hz, 2H), 2.52 (t, J=6.5 Hz, 2H), 1.61–1.43 (m, 2H), 1.37–1.14 (m, 2H), 1.05–0.73 (m, 1H). 13C NMR (75 MHz, DMSO-d_6) δ 203.33, 172.74, 64.77, 47.19, 34.94, 31.55, 28.72, 27.76, 25.68, 22.67, 14.58. LRMS, ESI:m/z 216.4 [M+H]+. HRMS: m/z calculated for $C_{11}H_{22}NO_3$ 216.1594 $[M+H]^+$, observed 216.1597.

Hexyl 5-((((4-(Methyl-(2,3,4-triacetyl-*β*-D-glucopyranuronate-1-yl)-3-nitrobenzyl)oxy) carbonyl) amino)-4-oxopentanoate (5). Compound **4** (20 mg, 41 µmol) and TEA (11.4 µL, 82 µmol) were dissolved in AcN (3.0 mL) and DMF (1.0 mL). *N,N′*-disuccinimidyl carbonate (15.8 mg, 62 µmol) was added and the reaction mixture stirred at ambient temperature for 1h. The reaction mixture was cooled

to 0 °C and hexyl 5-amino-4-oxopentanoate hydrochloride (21 mg, 83 µmol) and TEA (11.4 µL, 82 µmol) were added. After 1h at 0°C the temperature was allowed to rise to ambient. After stirring for 2 h DCM (20 mL) was added and the organic phase washed with diluted HCl (0.01 M, 2x5 mL). The organic phase was evaporated in vacuo and purified by Flash chromatography using hexane/ethyl acetate gradient yielding a yellow sticky solid (25 mg, 34 µmol, 82.9 %). ^{1}H NMR (600 MHz, $CDCl_3$) δ 7.82 (d, J = 2.2 Hz, 1H), 7.55 (dd, J = 8.6, 2.1 Hz, 1H), 7.38 (d, J = 8.5 Hz, 1H), 5.41 – 5.28 (m, 3H), 5.22 (d, J = 6.7 Hz, 1H), 5.12 (s, 2H), 4.23 (d, J = 8.9 Hz, 1H), 4.19 – 4.07 (m, 2H), 4.07 (d, J = 6.9 Hz, 2H), 3.76 (s, 3H), 2.74 (dd, J = 7.8, 5.7 Hz, 2H), 2.67 (dd, J = 7.1, 4.9 Hz, 2H), 2.14 (s, 3H), 2.08 (s, 3H), 2.06 (s, 3H), 1.62 (dq, J = 13.7, 6.1, 5.4 Hz, 2H), 1.32 (m, 6H), 0.90 (t, J = 6.8 Hz, 3H).^{13}C NMR (151 MHz, CDCl3) δ 203.53, 172.42, 170.02, 169.30, 169.24, 166.67, 155.59, 148.74, 141.21, 133.32, 132.86, 124.63, 120.13, 99.78, 72.57, 71.07, 70.14, 68.71, 65.13, 65.06, 53.07, 50.62, 34.39, 31.39, 28.51, 27.86, 25.52, 22.52, 20.60, 20.55, 20.52, 13.99. LRMS (ESI): m/z calculated for $[M+NH_4]^+$ 744.4, found 744.8. HRMS (ESI): m/z calculated for $C_{32}H_{42}N_2O_{17}$ $[M+NH_4]^+$ 744.2822, found 744.2831.

Hexyl 5-((((4-(β-D-glucuronyl)-3-nitrobenzyl)oxy) carbonyl)amino)-4-oxopentanoate (6). Compound **5** (100 mg, 0.138 mmol) was dissolved in a mixture of MeOH (65 mL), H_2O (20 mL) and TEA (650 µL). The reaction was stirred at 70 °C for 2 h and then concentrated under reduced pressure. The crude product was purified by RP-HPLC using H_2O/AcN gradient containing 0.01% TFA. The fractions containing the product were pooled and lyophilized giving colourless fluffy solid (63 mg, 0.104 mmol, 75.6 %). ^{1}H NMR (300 MHz, DMSO-d_6) δ 7.84 (d, J = 2.1 Hz, 1H), 7.65 – 7.55 (m, 2H), 7.41 (d, J = 8.8 Hz, 1H), 5.30 (d, J = 4.3 Hz, 1H), 5.10 (d, J = 7.6 Hz, 2H), 5.01 (s, 2H), 3.96 (t, J = 6.6 Hz, 2H), 3.86 (d, J = 5.9 Hz, 2H), 3.58 (d, J = 9.2 Hz, 1H), 3.26 – 3.11 (m, 4H), 2.66 (t, J = 6.5 Hz, 2H), 2.45 (d, J = 6.4 Hz, 2H), 1.52 (t, J = 7.3 Hz, 2H), 1.32 – 1.17 (m, 6H), 0.93 – 0.77 (m, 3H). ^{13}C NMR (151 MHz, MeOD) δ 205.50, 173.01, 170.46, 157.23, 149.21, 140.63, 132.94, 131.75, 124.04, 117.41, 100.94, 75.91, 75.23, 72.96, 71.27, 64.67, 64.49, 49.63, 33.58, 31.19, 28.25, 27.28, 25.26, 22.20, 12.94. LRMS (ESI): m/z calculated for $[M+H]^+$ 587.2, found 587.2. HRMS (ESI): m/z calculated for $C_{25}H_{34}N_2O_{14}$ $[M+NH_4]^+$ 604.2348, found 604.2358.

4.3. β-glucuronidase assay

Glu-ALA-Hex (0.05, 0.10 and 0.20 mM) was dissolved in phosphate buffer solution (25 mM) at pH 6.80. β-glucuronidase (11,458 U/mg) dissolved in the same buffer (100 U/mL stock solution) was added (1.0 U/mL) and the vial was placed in a temperature-controlled LC-MS auto-sampler preheated at 37 °C. Aliquots (5.0 µL) were injected at regular time points. Fast gradient mode of 30% A to 98% A in 3 min followed by 2 min equilibration at 400.0 µL/min and 40 °C column temperature was used (A =

CH_3CN, B = ammonium acetate (25 mM). The chromatograms were integrated and the amount of remaining Glu-ALA-Hex was determined and plotted as a function of time (N=3).

4.4. Chemical stability

The stability was assayed at pH 7.40. Glu-ALA-Hex or ALA-Hex were dissolved in phosphate buffer (25 mM) at 1.0 mM. The vial was placed in a temperature-controlled LC-MS autosampler preheated at 37 °C and injected at regular time points. UPLC chromatograms were integrated and the amount of the remaining compounds was determined and plotted as a function of time (N=3).

4.5. Cell culture

Human breast adenocarcinoma cell line MCF7 (ATTC® HTB-22TM, Manassas, Virginia) was grown in Minimum Essential Media (31095-029, Thermo Fisher Scientific) supplemented with 10 % fetal calf serum (CVFSVF00-01, Eurobio), and 1 % PenStrep (100 µL/mL streptomycin and 100 IU/mL penicillin, 15140-122, Thermo Fisher Scientific) in a humidified atmosphere containing 5 % CO_2 at 37 ^{0}C. Cells were routinely maintained by serial passage in fresh medium.

4.6. Dark toxicity

The dark toxicity assay was performed in MCF7 cells. The cell viability was tested by Cell Proliferation reagent (WST-1) using manufacturer's instructions (11644807001, Roche, Sigma-Aldrich, St. Gallen, Switzerland). Briefly, MCF7 cells (10^4 cells in 100 µL of full media) were seeded onto 96-well plate. The following day, the culture medium was changed and the cells were incubated for 4 h with ALA-Hex and Glu-ALA-Hex (0.1, 0.33, 1.0, 2.0, 3.3 mM) in the presence or absence of β-glucuronidase (1 U/mL) at 37 °C and 5 % of CO_2 in the dark. The absorption was measured at 450 nm with a plate reader (Safire, Tecan, Switzerland). The percentage of cell survival was calculated with a reference wavelength set at 680 nm for cells treated with either MEM medium (10% FCS, 1% PenStrep, 100 U/mL penicillin and 100 µg/mL streptomycin) or a solution of DMSO (50%). Mean values from three wells were determined and expressed as cell viability +/− s.d.

4.7. PpIX fluorescence kinetic measurements

PpIX fluorescence kinetic measurements were performed as described previously [14]. Briefly, human breast adenocarcinoma cell line MCF7 were seeded in 96-well plates (clear bottom black plate, 3603, Corning) at a density of 10^4 cells/well. The following day, PpIX fluorescence was recorded with a plate

reader (Safire, Tecan, Switzerland) at different time points upon the incubation with 0.10, 0.33, 1.00, 2.00 and 3.33 mM concentration of ALA-Hex or Glu-ALA-Hex in the presence or absence of β-glucuronidase (1 U/mL). Excitation wavelength for PpIX was set to 405 nm and emission wavelength to 630 nm. Mean values +/− s.d. for each concentration at each time point per plate were subtracted with the background fluorescence value (no treatment) and plotted as a function of time or concentration.

4.8. Confocal fluorescence microscopy

Human breast adenocarcinoma MCF7 cells (70,000 cells/well) were seeded into ibidi µ-Slides, ibiTreat, 4 (80426-IBI) wells 24 h before the experiment. In order to investigate the subcellular distribution of PpIX, cell monolayers were incubated for 4 h in the dark at 37°C with Glu-ALA-Hex (**6**) and ALA-Hex in complete medium. Cells of the control experiments were incubated in full medium under the same experimental conditions. Cells were then washed with DPBS and incubated for 10 min with 1 µg/mL Hoechst 33342 stain (62249, Thermo Fisher Scientific, Zug, Switzerland) and 30 min with 50 nM MitoTracker® Green FM (M7514 Thermo Fisher Scientific, Zug, Switzerland) or 70 nM of LysoTracker® Green DND-26 (8783 Thermo Fisher Scientific, Zug, Switzerland). Prior to imaging, cells were washed with complete medium. Detection and localization of PpIX fluorescence in live cells was done with the Zeiss LSM780 (Jena, Germany) inverted confocal microscope equipped with temperature, humidity and CO_2 control. The microscopic images were taken using 405 nm, 488 nm, 640 nm excitation lasers and 415 – 486 nm, 499 – 561 nm and 660 – 750 nm emission band filters, an objective lens CFI Plan-Aprochromat 60 x/1.4 oil. During the image acquisition time, slides were kept at 37°C in a humidified chamber. ImageJ software 1.51j8 (NIH, USA) was used for image processing.

Acknowledgements

We thank Dr. Francois Prodon from the Bioimaging Core Facility at the University of Geneva for his input and help with bioimaging experiments. We are grateful to Dr. Laurence Marcourt of the School of Pharmaceutical Sciences Geneva-Lausanne for her contribution in NMR experiments. We would also like to acknowledge the Mass Spectrometry platform at the University of Geneva for the mass spectroscopy analysis. We thank Canton of Geneva, Switzerland and Swiss National Science Foundation for funding. This work was supported by the Swiss National Science Foundation (grant 205321_173027).

Declaration of interest: none.

Appendix A. Supplementary material

Supplementary Information associated with this article can be found, in the online version, at https:// These data include ^{1}H, ^{13}C and MS spectra of all the compounds described in this article.

References

[1] A. Casas, C. Perotti, B. Ortel, G. Di Venosa, M. Saccoliti, A. Batlle, T. Hasan, Tumor cell lines resistant to ALA-mediated photodynamic therapy and possible tools to target surviving cells, International journal of oncology, 29 (2006) 397-405.

[2] M.J. Landau, D.J. Gould, K.M. Patel, Advances in fluorescent-image guided surgery, Ann Transl Med, 4 (2016).

[3] D.W. Roberts, P.A. Valdes, B.T. Harris, A. Hartov, X.Y. Fan, S.B. Ji, F. Leblond, T.D. Tosteson, B.C. Wilson, K.D. Paulsen, Glioblastoma Multiforme Treatment with Clinical Trials for Surgical Resection (Aminolevulinic Acid), Neurosurg Clin N Am, 23 (2012) 371-+.

[4] N. Lange, P. Jichlinski, M. Zellweger, M. Forrer, A. Marti, L. Guillou, P. Kucera, G. Wagnieres, H. van den Bergh, Photodetection of early human bladder cancer based on the fluorescence of 5-aminolaevulinic acid hexylester-induced protoporphyrin IX: a pilot study, Br J Cancer, 80 (1999) 185-193.

[5] K. Inoue, H. Fukuhara, T. Shimamoto, M. Kamada, T. Iiyama, M. Miyamura, A. Kurabayashi, M. Furihata, M. Tanimura, H. Watanabe, T. Shuin, Comparison between intravesical and oral administration of 5-aminolevulinic acid in the clinical benefit of photodynamic diagnosis for nonmuscle invasive bladder cancer, Cancer-Am Cancer Soc, 118 (2012) 1062-1074.

[6] Y. Murayama, D. Ichikawa, N. Koizumi, S. Komatsu, A. Shiozaki, Y. Kuriu, H. Ikoma, T. Kubota, M. Nakanishi, Y. Harada, H. Fujiwara, K. Okamoto, T. Ochiai, Y. Kokuba, T. Takamatsu, E. Otsuji, Staging Fluorescence Laparoscopy for Gastric Cancer by Using 5-Aminolevulinic Acid, Anticancer Research, 32 (2012) 5421-5427.

[7] N. Koizumi, Y. Harada, Y. Murayama, K. Harada, M. Beika, Y. Yamaoka, P. Dai, S. Komatsu, T. Kubota, D. Ichikawa, K. Okamoto, A. Yanagisawa, E. Otsuji, T. Takamatsu, Detection of metastatic lymph nodes using 5-aminolevulinic acid in patients with gastric cancer, Ann Surg Oncol, 20 (2013) 3541-3548.

[8] R. Vanseviciute, J. Venius, O. Zukovskaja, D. Kanopiene, S. Letautiene, R. Rotomskis, 5-Aminolevulinic-acid-based fluorescence spectroscopy and conventional colposcopy for in vivo detection of cervical pre-malignancy, Bmc Womens Health, 15 (2015).

[9] M. Loning, H. Diddens, W. Kupker, K. Diedrich, G. Huttmann, Laparoscopic fluorescence detection of ovarian carcinoma Metastases using 5-aminolevulinic acid-induced protoporphyrin IX, Cancer-Am Cancer Soc, 100 (2004) 1650-1656.

[10] H. Wang, Y. Yang, H. Chen, J. Dan, J. Cheng, S. Guo, X. Sun, W. Wang, Y. Ai, S. Li, Z. Li, L. Peng, Z. Tian, L. Yang, J. Wu, X. Zhong, Q. Zhou, P. Wang, Z. Zhang, W. Cao, Y. Tian, The predominant pathway of apoptosis in THP-1 macrophage-derived foam cells induced by 5-aminolevulinic acid-mediated sonodynamic therapy is the mitochondria-caspase pathway despite the participation of endoplasmic reticulum stress, Cell Physiol Biochem, 33 (2014) 1789-1801.

[11] J.T. Dalton, C.R. Yates, D. Yin, A. Straughn, S.L. Marcus, A.L. Golub, M.C. Meyer, Clinical pharmacokinetics of 5-aminolevulinic acid in healthy volunteers and patients at high risk for recurrent bladder cancer, J Pharmacol Exp Ther, 301 (2002) 507-512.

[12] N. Fotinos, M.A. Campo, F. Popowycz, R. Gurny, N. Lange, 5-Aminolevulinic acid derivatives in photomedicine: Characteristics, application and perspectives, Photochemistry and photobiology, 82 (2006) 994-1015.

[13] F. Giuntini, L. Bourre, A.J. MacRobert, M. Wilson, I.M. Eggleston, Improved Peptide Prodrugs of 5-ALA for PDT: Rationalization of Cellular Accumulation and Protoporphyrin IX Production by Direct Determination of Cellular Prodrug Uptake and Prodrug Metabolization, J Med Chem, 52 (2009) 4026-4037.

[14] A. Babič, V. Herceg, I. Ateb, E. Allémann, N. Lange, Tunable phosphatase-sensitive stable prodrugs of 5-aminolevulinic acid for tumor fluorescence photodetection, Journal of Controlled Release, 235 (2016) 155-164.

[15] V. Herceg, N. Lange, E. Allémann, A. Babič, Activity of phosphatase-sensitive 5-aminolevulinic acid prodrugs in cancer cell lines, Journal of photochemistry and photobiology. B, Biology, 171 (2017) 34-42.

[16] F.E. Brot, C.E. Bell, Jr., W.S. Sly, Purification and properties of beta-glucuronidase from human placenta, Biochemistry, 17 (1978) 385-391.

[17] K. Paigen, Mammalian beta-glucuronidase: genetics, molecular biology, and cell biology, Prog Nucleic Acid Res Mol Biol, 37 (1989) 155-205.

[18] W.H. Fishman, A.J. Anlyan, The presence of high beta-glucuronidase activity in cancer tissue, J Biol Chem, 169 (1947) 449.

[19] T.A. Connors, M.E. Whisson, Cure of mice bearing advanced plasma cell tumours with aniline mustard: the relationship between glucuronidase activity and tumour sensitivity, Nature, 210 (1966) 866-867.

[20] N. Albin, L. Massaad, C. Toussaint, M.C. Mathieu, J. Morizet, O. Parise, A. Gouyette, G.G. Chabot, Main drug-metabolizing enzyme systems in human breast tumors and peritumoral tissues, Cancer Res, 53 (1993) 3541-3546.

[21] K. Bosslet, R. Straub, M. Blumrich, J. Czech, M. Gerken, B. Sperker, H.K. Kroemer, J.P. Gesson, M. Koch, C. Monneret, Elucidation of the mechanism enabling tumor selective prodrug monotherapy, Cancer Res, 58 (1998) 1195-1201.

[22] M. de Graaf, E. Boven, H.W. Scheeren, H.J. Haisma, H.M. Pinedo, Beta-glucuronidase-mediated drug release, Curr Pharm Des, 8 (2002) 1391-1403.

[23] L.F. Tietze, R. Seele, B. Leiting, T. Krach, Stereoselective synthesis of (1-alkoxyalkyl) alpha- and beta-D-glucopyranosiduronates (acetal-glucopyranosiduronates): a new approach to specific cytostatics for the treatment of cancer, Carbohydr Res, 180 (1988) 253-262.

[24] P.H. Houba, E. Boven, C.A. Erkelens, R.G. Leenders, J.W. Scheeren, H.M. Pinedo, H.J. Haisma, The efficacy of the anthracycline prodrug daunorubicin-GA3 in human ovarian cancer xenografts, Br J Cancer, 78 (1998) 1600-1606.

[25] R.G.G. Leenders, E.W.P. Damen, E.J.A. Bijsterveld, H.W. Scheeren, P.H.J. Houba, I.H. van der Meulen-Muileman, E. Boven, H.J. Haisma, Novel anthracycline-spacer-beta-glucuronide, -beta-glucoside, and -beta-galactoside prodrugs for application in selective chemotherapy, Bioorgan Med Chem, 7 (1999) 1597-1610.

[26] P.H. Houba, E. Boven, I.H. van der Meulen-Muileman, R.G. Leenders, J.W. Scheeren, H.M. Pinedo, H.J. Haisma, A novel doxorubicin-glucuronide prodrug DOX-GA3 for tumour-selective chemotherapy: distribution and efficacy in experimental human ovarian cancer, Br J Cancer, 84 (2001) 550-557.

[27] M. Grinda, J. Clarhaut, I. Tranoy-Opalinski, B. Renoux, A. Monvoisin, L. Cronier, S. Papot, A heterodimeric glucuronide prodrug for cancer tritherapy: the double role of the chemical amplifier, ChemMedChem, 6 (2011) 2137-2141.

[28] E. Bouvier, S. Thirot, F. Schmidt, C. Monneret, A new paclitaxel prodrug for use in ADEPT strategy, Org Biomol Chem, 1 (2003) 3343-3352.

[29] A.E. Alaoui, N. Saha, F. Schmidt, C. Monneret, J.C. Florent, New Taxol (paclitaxel) prodrugs designed for ADEPT and PMT strategies in cancer chemotherapy, Bioorg Med Chem, 14 (2006) 5012-5019.

[30] R. Madec-Lougerstay, J.C. Florent, C. Monneret, Synthesis of self-immolative glucuronide spacers based on aminomethylcarbamate. Application to 5-fluorouracil prodrugs for antibody-directed enzyme prodrug therapy, J Chem Soc Perk T 1, (1999) 1369-1375.

[31] Y.L. Leu, S.R. Roffler, J.W. Chern, Design and synthesis of water-soluble glucuronide derivatives of camptothecin for cancer prodrug monotherapy and antibody-directed enzyme prodrug therapy (ADEPT), J Med Chem, 42 (1999) 3623-3628.

[32] Z.M. Prijovich, B.M. Chen, Y.L. Leu, J.W. Chern, S.R. Roffler, Anti-tumour activity and toxicity of the new prodrug 9-aminocamptothecin glucuronide (9ACG) in mice, Br J Cancer, 86 (2002) 1634-1638.

[33] T.Y. Juan, S.R. Roffler, H.S. Hou, S.M. Huang, K.C. Chen, Y.L. Leu, Z.M. Prijovich, C.P. Yu, C.C. Wu, G.H. Sun, T.L. Cha, Antiangiogenesis targeting tumor microenvironment synergizes glucuronide prodrug antitumor activity, Clin Cancer Res, 15 (2009) 4600-4611.

[34] Z.M. Prijovich, P.A. Burnouf, H.C. Chou, P.T. Huang, K.C. Chen, T.L. Cheng, Y.L. Leu, S.R. Roffler, Synthesis and Antitumor Properties of BQC-Glucuronide, a Camptothecin Prodrug for Selective Tumor Activation, Mol Pharmaceut, 13 (2016) 1242-1250.

[35] O.B. Gadmar, J. Moan, E. Scheie, L.W. Ma, Q. Peng, The stability of 5-aminolevulinic acid in solution, J Photoch Photobio B, 67 (2002) 187-193.

[36] J. Kloek, G.M.J.B. vanHenegouwen, Prodrugs of 5-aminolevulinic acid for photodynamic therapy, Photochemistry and photobiology, 64 (1996) 994-1000.

[37] Y. Berger, A. Greppi, O. Siri, R. Neier, L. Juillerat-Jeanneret, Ethylene glycol and amino acid derivatives of 5-aminolevulinic acid as new photosensitizing precursors of protoporphyrin IX in cells, J Med Chem, 43 (2000) 4738-4746.

[38] J. Moan, O. Bech, J.M. Gaullier, T. Stokke, H.B. Steen, L.W. Ma, K. Berg, Protoporphyrin IX accumulation in cells treated with 5-aminolevulinic acid: dependence on cell density, cell size and cell cycle, Int J Cancer, 75 (1998) 134-139.

[39] C.A. Blencowe, A.T. Russell, F. Greco, W. Hayes, D.W. Thornthwaite, Self-immolative linkers in polymeric delivery systems, Polym Chem-Uk, 2 (2011) 773-790.

[40] H.J. Haisma, M. van Muijen, H.M. Pinedo, E. Boven, Comparison of two anthracycline-based prodrugs for activation by a monoclonal antibody-beta-glucuronidase conjugate in the specific treatment of cancer, Cell Biophys, 24-25 (1994) 185-192.

[41] M. Azoulay, J.C. Florent, C. Monneret, J.P. Gesson, J.C. Jacquesy, F. Tillequin, M. Koch, K. Bosslet, J. Czech, D. Hoffman, Prodrugs of anthracycline antibiotics suited for tumor-specific activation, Anticancer Drug Des, 10 (1995) 441-450.

[42] R.G. Leenders, E.W. Damen, E.J. Bijsterveld, H.W. Scheeren, P.H. Houba, I.H. van der Meulen-Muileman, E. Boven, H.J. Haisma, Novel anthracycline-spacer-beta-glucuronide,-beta-glucoside, and -beta-galactoside prodrugs for application in selective chemotherapy, Bioorg Med Chem, 7 (1999) 1597-1610.

[43] F. Schmidt, J.C. Florent, C. Monneret, R. Straub, J. Czech, M. Gerken, K. Bosslet, Glucuronide prodrugs of hydroxy compounds for antibody directed enzyme prodrug therapy (ADEPT): A phenol nitrogen mustard carbamate., Bioorg Med Chem Lett, 7 (1997) 1071-1076.

[44] G.N. Bollenback, J.W. Long, D.G. Benjamin, J.A. Lindquist, The Synthesis of Aryl-D-Glucopyranosiduronic Acids, J Am Chem Soc, 77 (1955) 3310-3315.

[45] R.B. Greenwald, A. Pendri, C.D. Conover, H. Zhao, Y.H. Choe, A. Martinez, K. Shum, S.Y. Guan, Drug delivery systems employing 1,4-or 1,6-elimination: Poly(ethylene glycol) prodrugs of amine-containing compounds, J Med Chem, 42 (1999) 3657-3667.

[46] M.R. Mattern, G.A. Hofmann, R.M. Polsky, L.R. Funk, F.L. McCabe, R.K. Johnson, In vitro and in vivo effects of clinically important camptothecin analogues on multidrug-resistant cells, Oncol Res, 5 (1993) 467-474.

[47] F. Schmidt, I. Ungureanu, R. Duval, A. Pompon, C. Monneret, Cancer chemotherapy: A paclitaxel prodrug for ADEPT (antibody-directed enzyme prodrug therapy), Eur J Org Chem, (2001) 2129-2134.

[48] R. Woessner, Z. An, X. Li, R.M. Hoffman, R. Dix, A. Bitonti, Comparison of three approaches to doxorubicin therapy: free doxorubicin, liposomal doxorubicin, and beta-glucuronidase-activated prodrug (HMR 1826), Anticancer Res, 20 (2000) 2289-2296.

[49] M. de Graaf, E. Boven, H.W. Scheeren, H.J. Haisma, H.M. Pinedo, Beta-glucuronidase-mediated drug release, Curr Pharm Design, 8 (2002) 1391-1403.

[50] Q. Shi, G.R. Haenen, L. Maas, V.M. Arlt, D. Spina, Y.R. Vasquez, E. Moonen, C. Veith, F.J. Van Schooten, R.W. Godschalk, Inflammation-associated extracellular beta-glucuronidase alters cellular responses to the chemical carcinogen benzo[a]pyrene, Arch Toxicol, 90 (2016) 2261-2273.

[51] P.H. Houba, R.G. Leenders, E. Boven, J.W. Scheeren, H.M. Pinedo, H.J. Haisma, Characterization of novel anthracycline prodrugs activated by human beta-glucuronidase for use in antibody-directed enzyme prodrug therapy, Biochem Pharmacol, 52 (1996) 455-463.

[52] R. Chen, Z. Huang, G. Chen, Y. Li, X. Chen, J. Chen, H. Zeng, Kinetics and subcellular localization of 5-ALA-induced PpIX in DHL cells via two-photon excitation fluorescence microscopy, International journal of oncology, 32 (2008) 861-867.

[53] B.W. Pogue, C. Sheng, J. Benevides, D. Forcione, B. Puricelli, N. Nishioka, T. Hasan, Protoporphyrin IX fluorescence photobleaching increases with the use of fractionated irradiation in the esophagus, J Biomed Opt, 13 (2008).

[54] L. Rodriguez, H.S. de Bruijn, G. Di Venosa, L. Mamone, D.J. Robinson, A. Juarranz, A. Batlle, A. Casas, Porphyrin synthesis from aminolevulinic acid esters in endothelial cells and its role in photodynamic therapy, J Photoch Photobio B, 96 (2009) 249-254.